

Improved Performance in Long-pulse ELMy H-mode Plasmas with Internal Transport Barrier in JT-60U

N. Oyama, A. Isayama, T. Suzuki, Y. Koide, H. Takenaga, S. Ide, T. Nakano, N. Asakura,
H. Kubo, M. Takechi, Y. Sakamoto, Y. Kamada, H. Urano, M. Yoshida, K. Tsuzuki,
G. Matsunaga, C. Gormezano and the JT-60 Team

Japan Atomic Energy Agency, Naka, Ibaraki-ken, 311-0193 Japan

e-mail contact of main author: oyama.naoyuki@jaea.go.jp

Abstract. After installation of ferritic steel tiles (FSTs), fast ion losses due to toroidal field ripple have been reduced by $1/2 \sim 1/3$. The increase in absorbed power at same injection power can reduce the required number of NB units to sustain a given β_N , resulting in a better flexibility of torque input by increasing the available combination of tangential NB units. By making use of these advantages to sustain an internal transport barrier (ITB), the performance of long-pulse ELMy H-mode plasmas was improved in terms of sustained duration time for both high normalized beta (β_N) and high thermal confinement enhancement factor ($H_{H98(y,2)}$). High $\beta_N > 2.3$ together with $H_{H98(y,2)} \sim 1$ was sustained for 23.1s ($\sim 12\tau_R$) at $q_{95} \sim 3.3$, which also provide high $\beta_N \cdot H_{H98(y,2)} \geq 2.2$ and a bootstrap current fraction of 36%-45%. $\beta_N \cdot H_{H98(y,2)}$ of 2.0 was sustained for 28.6s, which is limited by the maximum injection period of 30s for NBI system. These long-pulse plasmas are possible candidates for ITER hybrid operation scenario. Improved confinement is characterized by the larger thermal components at a given density maintained by smaller heating power than in previous experiments. The strength of the ITB depends on the pedestal temperature, which varies with edge density while keeping constant the pressure (limited by type I ELMs). These long-pulse plasmas indicate that further investigation to establish high performance plasmas longer than τ_w with active particle control is essential to establish the operational scenarios for next step devices, where the wall pumping does not work.

1. Introduction

Beyond the ITER standard operation with high fusion gain (Q) of 10 for ~ 400 s, several advanced tokamak plasma operations have been proposed for ITER to extend the time duration of burning plasma toward steady-state operations. One of these advanced operational modes is the "hybrid scenario" [1, 2], where pulse duration is longer than ~ 1000 s thanks to non-inductive current drive and the subsequent reduced flux consumption providing larger neutron fluence per pulse. It has been developed in many tokamaks [3-6]. One of the key parameter in the "hybrid scenario" is a non-inductive current fraction of larger than 40%. Since such a large non-inductive current including the bootstrap current should be kept stationary throughout the discharge, a demonstration of high performance plasma with high bootstrap current much longer than the current diffusion time ($\tau_R \equiv \mu_0 \langle \sigma \rangle a^2 / 12$ [7]) is important to establish "hybrid scenario" in ITER.

In JT-60U, in order to expand the advanced tokamak (AT) plasma regime with time scales longer than τ_R , the control systems for operation, heating and diagnostics have been modified [6]. However, further pursuit of long sustainment of high performance plasmas has been handicapped by the loss of fast ions due to the toroidal field ripple from the viewpoint of the available net heating power and controllability of the toroidal rotation profile due to the formation of an inward electric field [8]. In order to reduce the toroidal field ripple, ferritic steel tiles (FSTs), which cover $\sim 10\%$ of the vacuum vessel surface, have been installed inside the JT-60U vacuum vessel on the low field side [9]. Making use of advantages of reduced fast ion losses after installation of FSTs, we have extended the sustainable duration of high β_N plasmas with better thermal plasma confinement and larger bootstrap current fraction (f_{BS}). In this paper, we report recent results of long-pulse AT research in JT-60U, which can contribute significantly towards the development of the ITER hybrid operation scenario.

2. Advantages of ripple reduction in long-pulse ELMy H-mode plasmas

The design of FSTs and its location are optimized to reduce the fast ion losses using Fully Three-Dimensional magnetic field Orbit Following Monte Carlo (F3D-OFMC) code. The 18-fold toroidal symmetry of the ripple amplitude was broken, because no FSTs were installed near the outer midplane in some toroidal sections due to limitation of space [9]. Here, "quasi" ripple well structure is defined by whether there is a local minimum of the magnetic field within $\phi_s - \Delta\phi < \phi < \phi_s + \Delta\phi$ at a given toroidal angle ϕ_s , where $\Delta\phi$ is half of the period of the TF coil installation [10]. Using this definition, figures 1(a) and 1(b) show a comparison of "quasi" ripple well structure without and with FSTs, respectively, based on plasma parameters and configurations in long-pulse ELMy H-mode plasmas at 1.6T. Although Fig. 1(b) is evaluated at a section, where the maximum local ripple exists, ripple well structure becomes small.

Calculated loss power of fast ions from perpendicular-(perp) NBIs reduces by 1/2~1/3 at 1.6T as shown in Fig. 1(c). Injection angles to the plasma in the toroidal direction for perp-NBIs are not fully at a right angle completely as shown in Fig. 1(d). It is noted that the loss power ratio of perp-NBIs is related to the tilted angle to the plasma current rather than to the beam trajectory (i.e. central heating for upper units and off-axis heating for lower units). Therefore, the selection of perp-NBIs is important to reduce the loss of fast ions.

The reduction of fast ion losses is the dominant effect in long-pulse ELMy H-mode experiments. The increase in absorbed power at same injection power can reduce the required number of NB units to sustain a given β_N , resulting in a better flexibility of torque input by increasing the available combination of tangential NB units. Since lower fast ion losses also reduced the formation of an inward electric field, plasma can now rotate in the same direction as the torque input from tangential NBIs [11].

3. Extension of sustained duration of high β_N plasmas

Making use of the advantages described in Sec. 2, the duration of high β_N plasmas has been extended close to the hardware limit of heating systems (30s for NBI system) in JT-60U. Figure 2 shows waveforms of a typical high β_N long-pulse plasma with the following parameters, $I_p=0.9\text{MA}$, $B_T=1.6\text{T}$, $q_{95}\sim 3.3$, $\delta\sim 0.32$ and $\kappa\sim 1.4$. Preheating from 2 tangential NBIs with balanced injection was applied during I_p ramp-up phase and gradually increased up

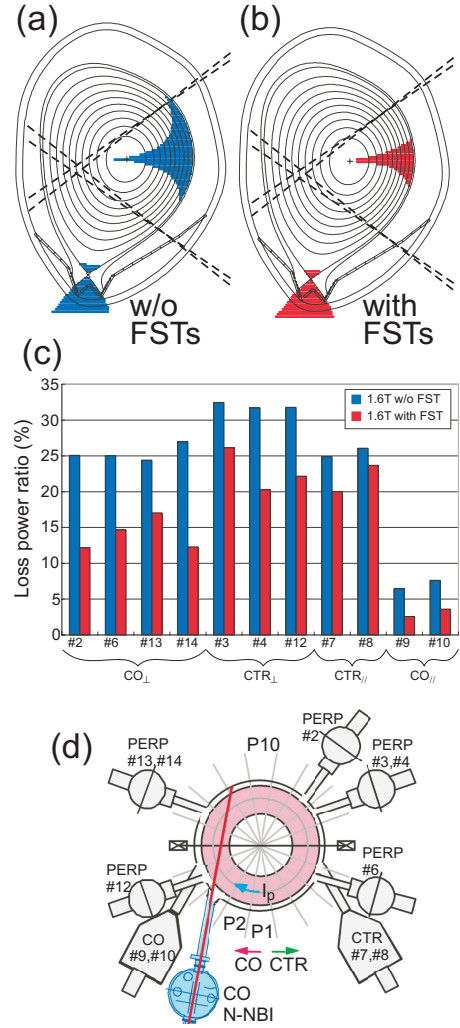


FIG. 1. "Quasi" ripple well structure (a) without and (b) with FSTs. The dashed lines show the beam trajectories of two ion sources from one perp-NBI unit. (c) Fast ion losses evaluated with F3D-OFMC code. Perp-NBIs of #2, 4, 6, 12, 14 and #3,13 are injected from upper and lower port, respectively. (d) Port arrangement of NBI system (top view).

to 8.1MW as shown in Fig. 2(a). A high confinement plasma ($H_{H98(y,2)} \sim 1.1$) with $\beta_N \geq 2.4$ was kept up to $t \sim 22$ s as shown in Fig. 2(b). Destabilization of neoclassical tearing modes (NTMs) was successfully avoided by optimizing the current profile and pressure profile [12] so that a steep pressure gradient is not located at the mode rational surfaces at $q=1.5$ and 2 as shown in Fig. 3(a). No detectable sawtooth activity was observed in this discharge, which was consistent with the time evolution of q profile (no $q=1$ surface or very narrow) as shown in Fig. 2(d). Such optimum q profile could be sustained much longer than τ_R (~ 2 s) with large f_{BS} of 36-45%, which is a consequence of the peaked pressure profile as shown in Fig. 3(a). On the other hand, there was an edge fluctuation with $m/n=3-4/1$ at ~ 4 kHz observed between type I ELMs as shown in Fig. 2(e). Here, m and n are poloidal and toroidal mode numbers, respectively. Nevertheless, the existence of edge fluctuations does not affect the plasma confinement, which was similar with and without this mode by changing the edge q profile with higher B_T .

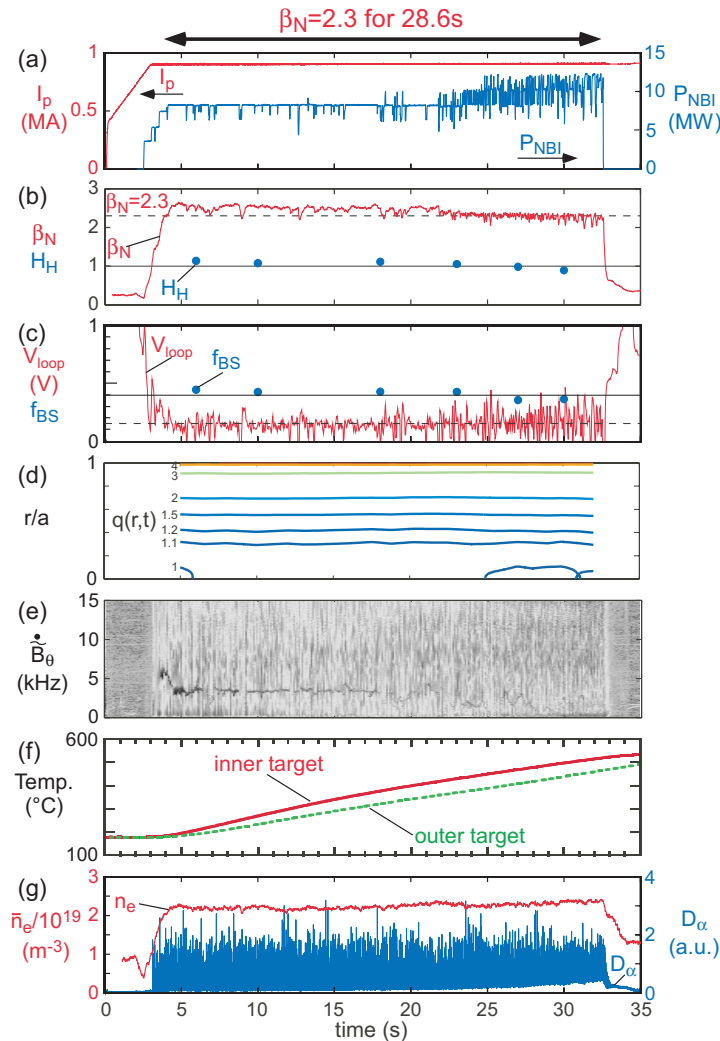


FIG. 2. Waveforms of a typical high β_N long-pulse plasma (E45436), (a) plasma current and heating power, (b) normalized beta, β_N , and confinement enhancement factor, $H_{H98(y,2)}$, (c) loop voltage and fraction of bootstrap current (d) safety factor, q , profile, (e) frequency spectrum of magnetic fluctuation (f) wall temperature at both inner and outer divertor target plates and (g) line-averaged density and divertor D_α intensity. Dashed line in (b) and (c) indicate $\beta_N=2.3$ and $V_{loop}=0.15$ V, respectively. Solid line in (b) and (c) indicate $H_H=1$ and $f_{BS}=0.4$, respectively.

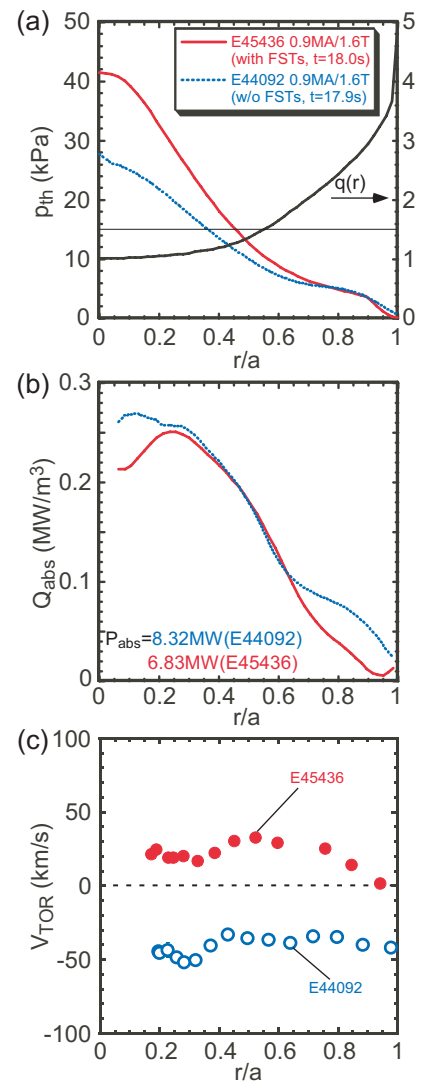


FIG. 3. Comparison of (a) thermal pressure profiles, (b) power deposition profile and (c) toroidal rotation profile in high β_N (>2.3), long-pulse plasma without FSTs (E44092 at 17.9s) and with FSTs (E45436 at 18.0s). Safety factor profile for E45436 is also shown in (a).

Because of the long duration of NB heating in these discharges, the surface temperature at the divertor targets continuously increased from $\sim 180^\circ\text{C}$ to $\sim 500^\circ\text{C}$ as shown in Fig. 2(f). The increase in wall temperature may increase the recycling level in the latter phase ($t > 23\text{s}$), as shown in Fig. 2(g), due to the reduced net pumping speed by the first wall [13]. During this phase, the core temperature, also in the ITB region, decreases with the reduction of edge temperature as the edge density increased, due to the core-pedestal interplay. These recycling effects on the plasma performance are described in Sec. 5. After switching from central heating to off-axis heating of perp-NBI at $t = 22.7\text{s}$ because of the limitation of available NB units, the power deposition profile became broader. Owing to these reasons, the same ITB performance could not be sustained in the latter phase ($t \sim 23\text{s}$). However, the constant stored energy feedback system increased the NB heating power to keep the stored energy at $\beta_N > 2.3$ throughout the discharge (28.6s). Then, the sustained duration of high β_N plasmas has been extended up, close to the limitation of the NB injection pulse length (30s) as shown in Fig. 4.

In the previous long-pulse ELMy H-mode experiments shown by open symbols in Fig. 4, the sustained duration of high β_N plasmas was limited by the maximum duration of the available power, mainly limited by 6 perp-NBIs for 10s injection. In E44092 ($t = 17.9\text{s}$) without FSTs, for example, average loss power of fast ions was 21.5% of injected power, while only 13.7% of injected power was lost in E45436 ($t = 18\text{s}$) with FSTs. Moreover, plasma confinement property in E45436 was much better than in E44092 as discussed in the next section. Then, we could reduce the number of NB units from 6-7 units (4 tangential NBIs plus some perp-NBIs and/or N-NBI) to 4.5-6.5 units (3.5 tangential NBIs plus one or two perp-NBIs) to sustain $\beta_N > 2.3$ resulting in longer sustained duration time without any modification of the heating system.

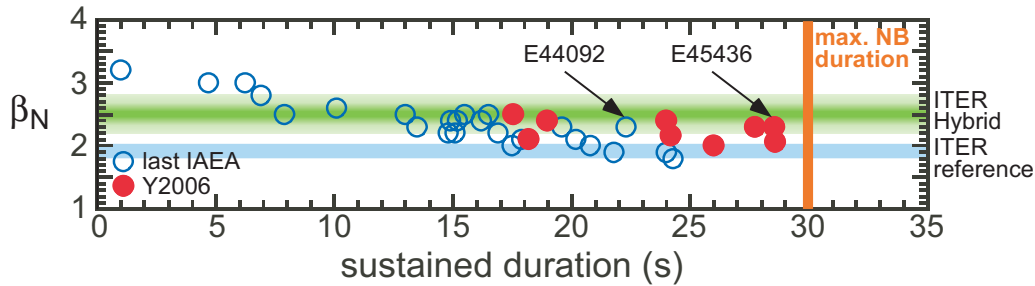


FIG. 4. Sustained duration of high β_N plasmas.

4. Improved thermal confinement in long-pulse plasma with high β_N

In addition to the extension of the sustained time duration of $\beta_N = 2.3$ for 6.3s as shown in Fig. 4, thermal confinement was much improved after installation of FSTs. Figure 3 shows the comparison of pressure profile, power deposition profile and toroidal rotation profile between two plasmas with similar achieved β_N , E44092 without FSTs and E45436 with FSTs. The ITB was formed in both plasmas with similar location of ITB foot. Nevertheless, the ITB performance was quite different with similar pedestal pressure. It is noted that the deposited power inside the ITB region was very similar for the two plasmas. Higher pressure profile sustained by smaller heating power as shown in Fig. 3(b) provides higher $H_{H98(y,2)}$ of 1.1 in E45436 with FSTs as compared to 0.82 in E44092 without FSTs.

Some part of this improvement of the ITB performance shown in Fig. 3(a) comes from the difference in the pedestal density and temperature as discussed in the next section. But, even when we compare the temperature profiles at the same pedestal density, ITB strength was different especially for the T_e -ITB. Figure 5(a) shows the density dependence of $H_{H98(y,2)}$ with and without FSTs. Higher $H_{H98(y,2)}$ can be obtained in all density region. The reason why plasmas with smaller $H_{H98(y,2)}$ could achieve similar β_N to those with FSTs is shown in Fig. 5(b). In the previous experiments without FSTs, the stored energy of the beam component

was higher than the thermal component. On the other hand, with FSTs, higher thermal component than the beam component was obtained at the similar β_N , resulting in a better thermal confinement.

As shown in Fig. 3(c), a larger co-toroidal rotation was observed with net co-torque input with FSTs. The effect of different toroidal rotation profile on the ITB performance was also investigated by changing the combination of tangential and perp-NBIs. As a result, we found that the reducing co-toroidal rotation has degraded the performance of T_e -ITB. Moreover, when we set the similar core toroidal rotation profile to the previous experiments without FSTs, achieved T_e profile became also similar. The better quality of T_e -ITB obtained in co-rotating plasmas with FSTs also gives some contribution to the improved performance in these long-pulse plasmas with high β_N .

Because of these improved thermal confinement, we could expand the operation regime toward higher $\beta_N \cdot H_{98(y,2)}$, which is a measure of fusion performance, for longer duration as shown in Fig. 6. In the discharge shown in Fig. 2, high $\beta_N \cdot H_{98(y,2)} \geq 2.2$ was sustained for 23.1s, which corresponds to $> \sim 12\tau_R$, with bootstrap current fraction of 36%-45%. Since these plasmas were operated in lower $q_{95} \sim 3.3$, a figure of merit for Q, so-called G-factor ($\beta_N \cdot H_{98(y,2)} / q_{95}^2$), has exceeded the value for ITER reference scenario of 0.2. Considering these plasma parameters, these discharges are possible candidates for ITER hybrid operation scenarios.

In order to evaluate the pedestal contribution to these higher thermal stored energy component, a relation between the pedestal β_p , $\beta_{p,ped}$, and the total β_p (a measure of Shafranov shift) is compared with the previous JT-60U database [14] in Fig. 5(c). Since the achieved β_N was similar in both long-pulse plasmas with similar q_{95} , achieved β_p was also similar. The fact that both long-pulse plasmas with (E45436) and without (E44092) FSTs achieved similar $\beta_{p,ped}$ at given β_p indicates that the improved thermal stored energy was mainly attributed to the improved ITB performance, as can be seen in Fig. 3(a).

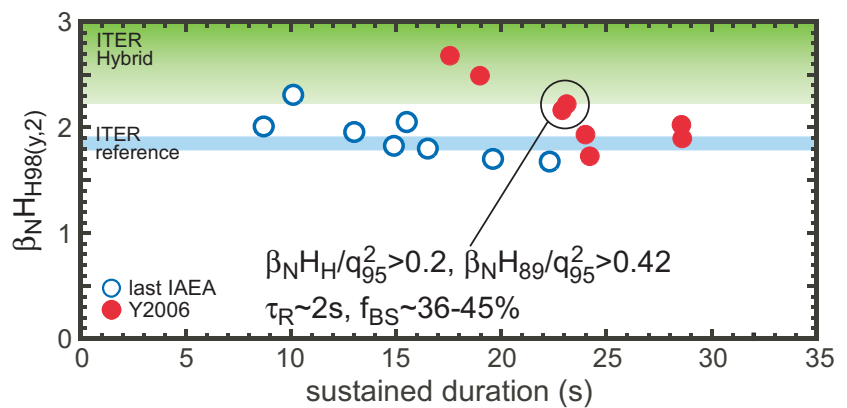


FIG. 6. Sustained duration of $\beta_N \cdot H_{98(y,2)}$.

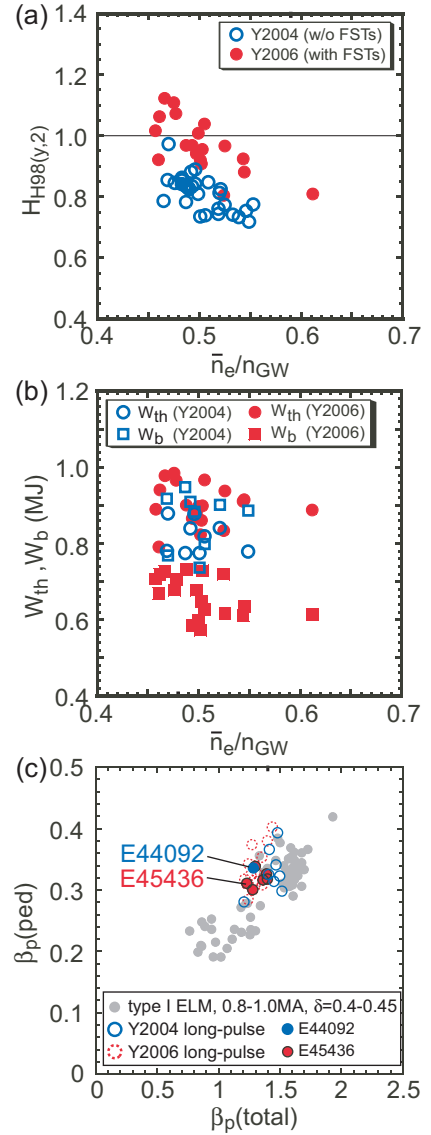


FIG. 5. Comparison of density dependence of (a) thermal confinement enhancement factor and (b) thermal and beam stored energy components. (c) relation between pedestal and total β_p . Type I ELM data shown by gray symbols indicate both with and without ITB.

5. Importance of particle control on ITB performance

The performance of these long-pulse plasmas degraded as the density and the recycling became higher in the latter phase as described in the previous section. It is important to understand the reason for the confinement degradation for the further development of long-pulse AT plasmas.

Figure 7(a) shows the pedestal operational regime in ion and electron including the time evolution of n_i - T_i trace for E45436. It is noted that the pedestal pressure for both ion and electron in these long-pulse plasmas were limited at $\sim 2\text{kPa}$ by type I ELMs. Therefore, the pedestal temperature has to vary to keep constant the pedestal pressure, similar to the usual type I ELMy H-mode plasmas without an ITB [15]. In E45436, the pedestal T_i started to decrease at $t \sim 23\text{s}$ due to the increase in the edge density. When the pedestal density increased by $\sim 30\%$ from 6s to 30s, the pedestal temperature also decreased by $\sim 30\%$ as shown in Fig. 7(a).

Pedestal temperature is quite important as a boundary condition for the core plasma in the ELMy H-mode plasmas due to the stiff-profile nature [15] in the temperature profile. Figure 7(b) shows the comparison of T_i profile between 6s and 30s. When the pedestal temperature decreased due to the increase in the edge density, core T_i including ITB region decreased with keeping constant $\nabla(\ln T_i)$. On the other hand, central n_e was unchanged, when the pedestal density increased, as shown in Fig. 7(c). The broader n_e profile caused smaller pressure profile, resulting in the confinement degradation in these long-pulse plasmas.

The power deposition profile at two time slices for the comparison of T_i and n_e profiles in Fig. 7 were different due to the higher heating power by about 2MW at 30s. In order to separate the effect of the recycling on the plasma performance from the different power deposition profile, two plasmas with different recycling condition, a low recycling case (E45436) and a high recycling case (E45570), are compared in Fig. 8. In high recycling case, higher heating power by $\sim 0.9\text{MW}$ (Fig. 8(f)) was applied in the early phase to achieve the same β_N . Then, the β_N increased up to similar level to the low recycling case, but the confinement degraded much faster than in the low recycling case, as shown in Fig. 8(e). The time evolutions of pedestal and core T_i are compared in Fig. 9(a). It is noted that the time evolution of core T_i follows the same line including ITB region, indicating the constant $\nabla(\ln T_i)$ between two plasmas. When we compare the pedestal density and temperature between two time slices at the same recycling with similar power deposition profile ($P_{\text{NET}} \sim 7.6\text{MW}$), $t=14\text{s}$ for E45570 and $t=27\text{s}$ for E45436, achieved pedestal density was similar, resulting in the similar temperature profile as shown in Fig. 9(a). As a result, achieved thermal pressure was also similar as shown in Fig. 9(b). On the other hand, when we

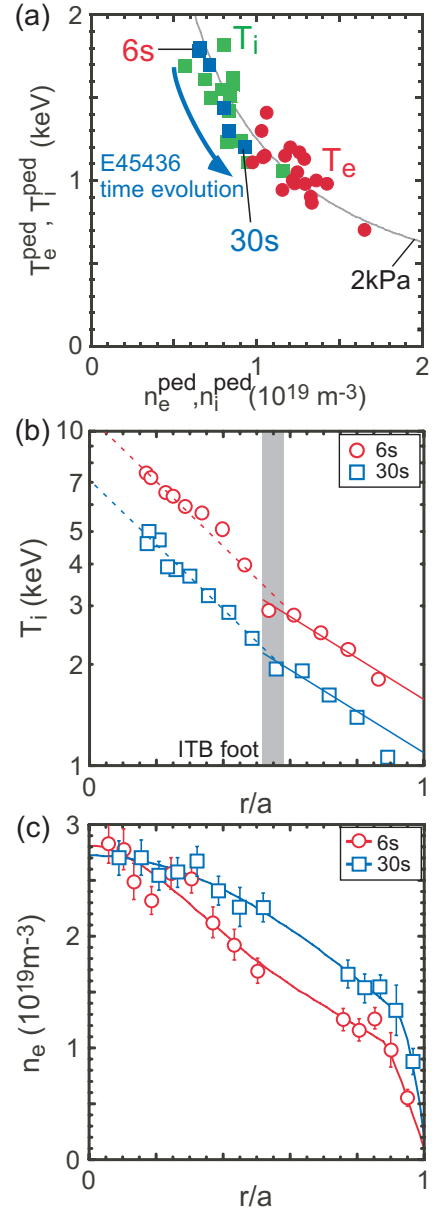


FIG. 7. Pedestal operational space in n_i - T_i and n_e - T_e . n_i was evaluated assuming that carbon is the only impurity. All data are taken with FSTs. (b) ion temperature profile and (c) density profile in E45436 at $t=6\text{s}$ and 30s .

compare two time slices at different recycling with similar power deposition profile, achieved pressure in high recycling case was smaller than that in low recycling plasma due to higher edge density. Therefore, higher edge density due to high recycling prevented a peaked pressure profile through the pedestal-core interplay, resulting in the degradation of the plasma confinement in these long-pulse plasmas.

From the viewpoint of the particle control in JT-60U, the condition of first wall as a pumping is quite important to obtain high performance plasmas. Even in such a long-pulse discharge, most of the injected particles were pumped out not by the divertor pumping but by the wall as shown in Fig. 8(b), when the wall inventory was small enough before the discharge. However, pumping speed of the wall became smaller in the latter phase of the discharge as the wall temperature increased with time, and then the divertor recycling and edge density slightly increased. When we repeated this kind of long-pulse discharges, such low recycling condition could not be kept any longer, and then finally the number of particles absorbed by the wall was effectively saturated even during the discharge as shown in Fig. 8(c). Because of the higher edge density in such wall condition with higher recycling, good ITB cannot be formed from the beginning of the discharge even if the heating power increased, as observed in Fig. 9(a) as the different highest temperature, $\sim 7\text{keV}$ in E45436 and $<6\text{keV}$ in E45570 at $r/a \sim 0.22$.

When the recycling level was high, such as in E45570, higher NB power cannot help to keep the high β_N plasma for long time, because higher NB power provides faster increase in divertor recycling due to larger fueling into the torus and larger heat flux to the wall, as shown in Fig. 8. Therefore, enough pumping

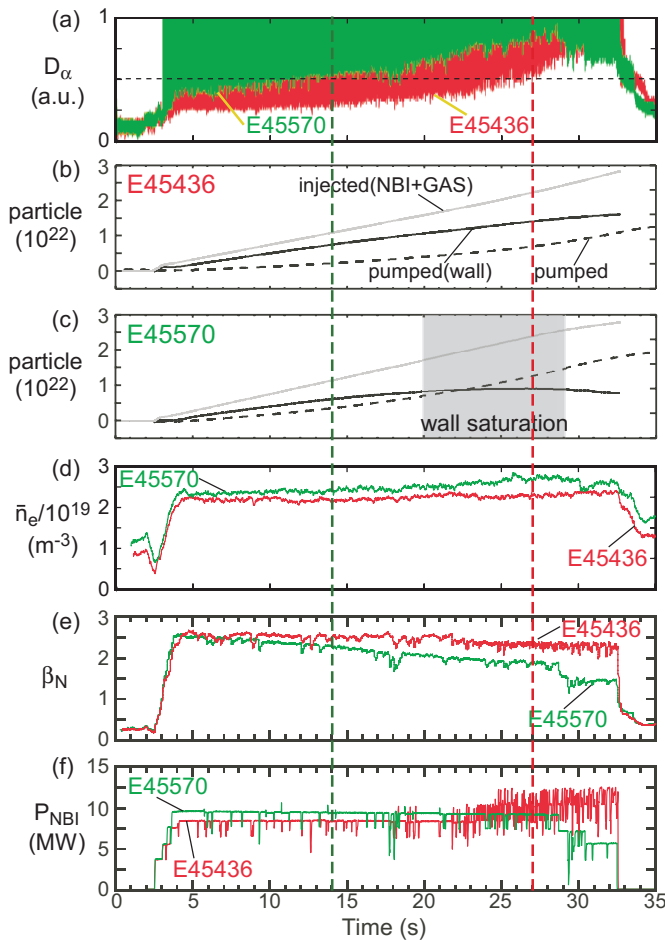


FIG. 8. Comparison of waveforms between low recycling (E45436) and high recycling (E45570) plasmas. (a) expanded divertor D_α intensity. (b), (c) particle balance for low and high recycling cases, respectively. (d) line-averaged density. (e) normalized beta, β_N . (f) heating power.

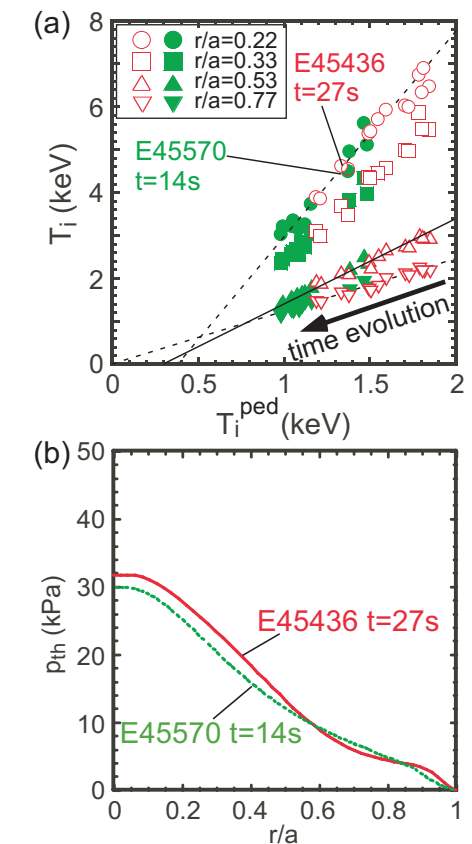


FIG. 9 (a) Time evolution and its relation between pedestal T_i and core T_i . (b) comparison of pressure profile.

capability to control the edge density is essential for keeping the long-pulse plasmas stationary longer than the time scale of wall saturation (τ_w). In JT-60U, however, the divertor pumping is effective only in high density plasmas with high divertor pressure under optimum configuration, where both divertor legs located close to divertor slot [16]. Therefore, wall conditioning is the only way to obtain enough pumping capability in these long-pulse experiments in JT-60U so far. These results indicate that further investigation to establish high performance plasmas longer than τ_w with active particle control is quite important to establish the operational scenarios for ITER and DEMO, where the wall pumping does not work.

6. Summary

After the installation of FSTs in JT-60U, fast ion losses due to toroidal field ripple have been reduced by 1/2~1/3 at 1.6T. The increase in absorbed power at same injection power can reduce the required number of NB units to sustain a given β_N , resulting in better flexibility of torque input by increasing the available combination of tangential NB units. Making use of these advantages to sustain good ITB, sustained duration of $\beta_N=2.3$ has been extended to 28.6s. In this plasma, smaller heating power could keep peaked pressure profile without NTMs and detectable sawteeth throughout the discharge. The improved core confinement provided high $\beta_N \cdot H_{98(y,2)} > 2.2$ with bootstrap current fraction of 36%-45% sustained for 23.1s ($\sim 12\tau_R$) at $q_{95} \sim 3.3$, which gives high G-factor (larger than 0.2). Therefore, these long-pulse plasmas are possible candidates for the ITER hybrid operation scenario. These long-pulse plasmas revealed the mechanism of ITB degradation due to the pedestal and core interplay. As the edge temperature decreased by increasing the edge density due to higher recycling, core T_i including inside ITB region degraded. It is now recognized that the controllability of the edge density and recycling level is quite important to keep the ITB performance in the long-pulse plasmas. Therefore, further investigation to establish high performance plasmas longer than τ_w with active particle control is essential to establish the operational scenarios for next step devices such as ITER and DEMO.

Acknowledgement

The authors acknowledge the members of the Japan Atomic Energy Agency who have contributed to the JT-60U projects. The authors are grateful to Dr. M. Kikuchi for continuous encouragement and support. This research was partly supported by the Grant-in-Aid for Young Scientists (A) 18686076, Japan Society for the Promotion of Science.

References

- [1] Green B. J. 2003 *Phys. Plasma Phys. Control. Fusion* **45** 687.
- [2] Sips A. C. C. 2005 *Phys. Plasma Phys. Control. Fusion* **47** A19.
- [3] Wade M. R. *et al.* 2005 *Nucl. Fusion* **45** 407.
- [4] Staebler A. *et al.* 2005 *Nucl. Fusion* **45** 617.
- [5] Joffrin E. *et al.* 2005 *Nucl. Fusion* **45** 626.
- [6] Ide S. and the JT-60 Team 2005 *Nucl. Fusion* **45** S48.
- [7] Mikkelsen D. R. 1989 *Phys. Fluids B* **1** 333.
- [8] Koide Y. *et al.* 1993 *Plasma Phys. Control. Nucl. Fusion Research* **1** 777.
- [9] Sakurai S. *et al.* 2006 submitted to *J. Nucl. Mater.*
- [10] Shinohara K. *et al.* 2006 *Plasma Fusion Res.* **1** 007.
- [11] Yoshida M. *et al.* 2006 to appear in *Phys. Plasma Phys. Control. Fusion.*
- [12] Isayama A. *et al.* 2003 *Nucl. Fusion* **43** 1272.
- [13] Nakano T. *et al.*, 2006 submitted to *J. Nucl. Mater.*
- [14] Kamada Y. *et al.* 2006 *Phys. Plasma Phys. Control. Fusion* **48** A419.
- [15] Urano H. *et al.* 2002 *Nucl. Fusion* **42** 76.
- [16] Kubo H. *et al.* 2006 Proc. 21st Int. Conf. on Fusion Energy 2006 (Chengdu, 2006)